Desalination and Water Treatment
www.deswater.com

doi: 10.1080/19443994.2014.956345

56 (2015) 1839–1854
November

Taylor & Francis
Taylor & Francis Group

Modelling of As^{3+} adsorption from aqueous solution using *Azadirachta indica* by artificial neural network

D. Gnanasangeetha[a,b,*], D. SaralaThambavani[b]

[a]*Department of Chemistry, PSNA College of Engineering and Technology, Dindigul, Tamilnadu, India, Tel. +9788742883; email: sangithprakash@yahoo.co.in (D. Gnanasangeetha)*
[b]*Research and Development Centre, Bharathiar University, Coimbatore, Tamilnadu, India, email: sarala_dr@yahoo.com (D. SaralaThambavani)*

Received 4 March 2014; Accepted 9 August 2014

ABSTRACT

An intensive study has been made on the removal efficiency of As^{3+} from aqueous solution by zinc oxide nanoparticle entrenched on activated silica (ZnO-NPs-AS) using aqueous leaf extract of *Azadirachta indica*. ZnO-NPs-AS is characterized using SEM-EDX, FT-IR and XRD. The effect of various parameters such as initial concentration of As^{3+}, adsorbent dosage, contact time, pH and agitation is studied systematically. The maximum adsorption of As^{3+} is found to be 98.31% at pH 5, equilibrium time of 50 min using adsorbent of 3 g/L and initial concentration of 0.06 mg/L at agitation speed of 250 rpm. Adsorption parameters for the Langmuir, Freundlich, Tempkin and BET isotherms were determined. The equilibrium data were best described by Langmuir isotherm model and fits quite well with the experimental data with good correlation coefficient of 0.974. The results of intraparticle diffusion model suggested that intraparticle diffusion was not the rate-controlling process. From the values, it is accomplished that the maximum adsorption corresponds to a saturated monolayer of As^{3+} molecules on the adsorbent surface with constant energy. The data were analysed using kinetics models akin to pseudo-first and second order. All the findings presented in this study suggested following pseudo-second-order equation for the adsorption of As^{3+} on to Zno-NPs-AS. The data collected from laboratory-scale experimental set up are used to train a feed forward back propagation learning algorithm having 5-20-1 three-layered architecture. The model uses tangent sigmoid transfer function at input to hidden layer whereas a linear purelin function is used at output layer. The data are divided into training (70%), testing (15%), and validation (15%) sets. The network is found to be working satisfactorily as absolute mean square percentage error of 0.0014 is obtained during training phase. Comparison between the model results and experimental data gives a high degree of correlation (R^2 = 0.986) indicating that the matlab nntool 2010a neural network model is able to predict the sorption efficiency with reasonable accuracy.

Keywords: Azadirachta indica; Artificial neural network; Adsorption; Modeling; ZnO-NPs-AS

*Corresponding author.

1. Introduction

The heavy metal arsenic is one of the most important pollutants which is mobilized by natural and anthropogenic processes like biological activity, geochemical reactions, volcanic eruption, mining activities and burning of fossil fuel. These activities contribute to contamination of water resources. Arsenic exists both in inorganic as well as organic forms in the water environment. Inorganic arsenic can occur in several forms e.g. metalloid arsenic As(0), As(III) (arsenites AsO_3^{2-}), and As(V) (arsenates, AsO_4^{3-}) but arsenic exists in two oxidation states in natural waters +3 and +5. Trivalent arsenic includes $As(OH)_3$, $As(OH)_4^-$, $AsO_2(OH)^{2-}$, and AsO_3^{3-}. It has been reported that the arsenic poisoning causes melanosis, oedema, keratosis, dark spots on the chest, enlargement of liver, kidney and spleen, cancers in skin, lung, urinary bladder and kidney [1–5]. Therefore, World Health Organization (WHO) has recommended the standard concentration of arsenic in drinking water as 10 mg/L. But it was observed that the typical arsenic concentration in arsenic-contaminated water used for human consumption is about 100–300 g/L [6,7]. Many methods have been proposed for removal of excessive As^{3+} from wastewater such as adsorption, coagulation, ion exchange, precipitation, electrolysis and reverse osmosis [8–14]. Most of these methods suffer from some disadvantages such as high capital and operational cost, limited tolerance to pH change, incomplete metal removal and high cost of reagent and energy requirements. Adsorption technique is quite trendy due its simplicity and high efficiency, as well as the ease of use of a wide range of adsorbents [15]. Adsorption has been treated as a potential technology for removal of toxic heavy metals from industrial waters using microbial biomass [16–19]. The main advantages of this technique are the reusability of biomaterial, low operating cost, improved selectivity for specific metals of interest, removal of heavy metals from effluent irrespective of toxicity, short operation time and no production of secondary compounds which might be toxic [20,21]. Preceding studies with established technical approaches are reported for the amputation of arsenic using Zirconium(IV) monophosphonic acid resin, Polyamide composite nanofiltration membranes and Fe(II)-loaded and Fe(III)-loaded apricot stone-based ACs, used as a biomaterial for the removal of As(V) and As(III), As(V) – at a pH of 3.0–7.0, 3–10 using column and membrane studies [22–24] and other sources of adsorption have been represented in Table 1.

The evolution of green chemistry in the production of nanoparticles has wrapped up an immense consideration because traces of chemicals left unreacted in the chemical synthesis process can be precarious. Owing to copious interest a competent protocol for the production of zinc oxide nanoparticle entrenched on activated silica (ZnO-NPs-AS) without calcinations was developed by green synthesis method using aqueous leaf extracts of *Azadirachta indica*. The aqueous leaf extract acts as a solvent with manifold roles as promoter, stabilizer and template for the synthesis of nanoparticle [25]. The qualitative examination of the aqueous extracts of the leaf sample of *A. indica* showed the presence of phytochemical constituents such as Alkaloid, Carbohydrate, Glycoside, Steroid, Flavonoid, Terpenoid, Tannins, and Steroid. The plant phytochemicals like terpenoids, flavonoids, alkaloids present in the aqueous leaf extract with antioxidant property were accountable for the preparation of zinc oxide nanoflowers [26,27]. Green synthesis and the biogenic green fabrication of *Azadirachta* are better due to its morphology, particle size and crystallinity. In this context, aqueous plant leaf extract of *A. indica* has been used to synthesize and found to be the best stabilizer for synthesizing ZnO NPs without the involvement of synthetic chemicals. And the study was further initiated and reported that ZnO-NPs-AS can be used as an inexpensive and effective adsorbent for the removal of arsenic ions from aqueous solution. This approach offers environmentally beneficial alternatives to more hazardous chemicals and processes and promotes pollution prevention by the production of nanoparticle in their natural environs. Over the years, many adsorption isotherm systems and kinetics have been modelled using equations include Langmuir, Freundlich, Intraparticle diffusion, pseudo-first-order and pseudo-second-order isotherm and kinetic models [28,29]. Although this classic adsorption isotherm, kinetic models are capable of representing certain equilibrium data-sets by themselves, they also display a considerable lack of fit when modelling non-traditional systems. The variable nature of these adsorption isotherms presents a challenge to the development of an equation that can be used to model the behaviour of all adsorption systems. Feed Forward Neural Networks (FFNNs) have been successfully used in many applications related to predict the pollutant removal efficiency based on a large data bank of pollutants, adsorption data for isopropanol–water system, adsorption from physical characteristics of activated carbons, volatile organic compound molecular properties and to model the equilibrium data of hydrogen onto activated carbons [30–32]. There is a vital requirement for development of innovative but low-cost processes by which heavy metals can be removed. The foremost advantage of an adsorption system of silica-embedded zinc oxide

Table 1
Various hybrid materials/composites and their arsenic removal capacities obtained

Sl. no.	Different hybrid materials	Adsorption capacity/density/ percentage	Ions removed	Methods used	Isotherm supported	References
1	Fe(III)/La(III)-chitosan	109 mg/g	As(III) and As (V)	Adsorption	–	[33]
2	Hybrid (polymeric/inorganic), fibrous sorbent, (FIBAN-As)	75.67 mg/g, 81.66 mg/g	As(III) and As (V)	Adsorption	Langmuir	[34]
3	Fe(II) loaded and Fe(III) loaded apricot, stone-based ACs	2.023 mg/g, 3.009 mg/g	As(III) and As (V)	Adsorption	Freundlich and Dubinin–Radush-kevich	[35]
4	GFH (granular ferric hydroxide)	6 8 mg/g	As(III)	Adsorption	Freundlich	[36]
5	Zinc oxide nanoparticle entrenched on activated slica	98.31%	As(III)	Adsorption/ kinetics	Langmuir and pseudo second order	Current material

Table 2
Experimental details of ZnO-NPs-AS for adsorption of As^{3+}

Effect of the System	Concentration (*N*)	Adsorption dosage (g)	Contact time (min)	pH	Agitation (rpm)
Concentration (N)	0.005, 0.0075, 0.01, 0.02, 0.03, 0.04, 0.05, **0.06**, 0.07, 0.08	0.06	50	5	250
Adsorption dosage (g)	0.06	0.5, 1, 1.5, 2, 2.5, **3,** 3.5, 4, 4.5	50	5	250
Contact time (min)	0.06	3	10, 20, 30, 40, **50,** 60, 70, 80	5	250
pH	0.06	3	50	1, 2, 3, 4, **5**, 6, 7	250
Agitation (rpm)	0.06	3	50	5	50, 100, 150, 200, **250**, 300, 350, 400

Note: Constant terms are represented in bold.

nanoparticle is less investment in terms of both initial cost and simple designed easy operation and has no effect of toxic substance compared to conventional chemical treatment process. Increasing awareness towards green chemistry and biological processes has led to the efficacy and feasibility of an eco-friendly approach for the synthesis of ZnO nanoparticle entrenched on activated silica as proficient adsorbent for removal of As (III) using artificial neural network (ANN). The scope of this paper is, therefore, to examine a single ANN structure can be used as a suitable comprehensive adsorption model to represent adsorption data where only the parameters of the fixed-structure model will change such that one will not have to search for the most appropriate structure of the model (Langmuir, Freundlich, Intraparticle diffusion, pseudo-first-order …) as it is currently being done in practice. It is basically a FFNN. It has a multi-layer structure consisting of one input and output layer and at least one hidden layer in between them. The number of nodes in input and output layers is decided by the number of independent and dependent parameters defining the process whereas the selection of number of hidden layers is dependent on the complexity of the process. The nodes in successive layers are interconnected with each other through connectionist constants called as weights. The data are transferred in the form of array of matrix from input layer to output layer through hidden layers. The output signal is compared to the target value to generate error signal.

Training of the network is to be carried out to minimize the error by adjusting the weights using appropriated algorithm [37,38].

2. Materials and methods

2.1. Preparation of ZnO-NPs-AS

Zinc acetate dihydrate (99% purity) and sodium hydroxide (pellet 99%) were used as the preparatory material and supplied by Sigma-Aldrich chemicals, India. ZnO-NPs-AS structure was primed by green synthesis method. Aqueous leaf extract of *A. indica* was stirred for 30 min to that 1 g of zinc acetate dihydrate was added under vigorous stirring. After 1hr stirring, 10 g of activated silica was introduced into the above solution followed by the addition of aqueous NaOH resulted in a white aqueous solution at pH 12. This was then sited in a magnetic stirrer for 2hr. The activated silica supported ZnO nanoparticle was then filtered and washed with double distilled water. The synthesized ZnO-NPs-AS was maintained at 60˚C for 12 h. A mortar was used to homogeneously ground the ZnO-NPs entrenched on activated silica. The proposed sorbent was stored in air at room temperature. The X-ray powder diffraction pattern of the as- synthesized sample was recorded on an X-ray diffractometer (XRD, PW 3040/60 Philips X'Pert, Holland) using Cu (Kα) radiation (λ = 1.5416 Å) operating at 40 kv and 30 mA with 2θ ranging from 10 to 90˚. The external morphology of the sample was characterized by scanning electron microscope (SEM) (LEO 1530FEGSEM).

2.2. Experimental details

The experiments were carried out as shown in Table 2. The effect of five parameters such as As^{3+} metal Concentration, Adsorbent dosage, Contact time, pH and Agitation speed was studied. To study the effect of certain parameter that has been changed progressively keeping the other four constant. The quantity of As^{3+} adsorbed by ZnO-NPs-AS was calculated using the following formulae.

$$\%\,\text{Removal} = (C_0 - C_e) \times 100/C_0 \tag{1}$$

$$q_e = (C_0 - C_e) \times V/W \tag{2}$$

where C_0 and C_e are initial and equilibrium concentration of As^{3+}, respectively, q_e is the amount of arsenic adsorbed, V is the volume of the solution and W is the weight of the adsorbent used.

2.3. Adsorption isotherm

Equilibrium data commonly known as adsorption isotherm describe how the adsorbate interacts with adsorbent and give a comprehensive understanding of the nature of interaction. It is basically important to optimize the design of adsorption system. The parameter obtain from different models provide important information on the surface properties of the adsorbent and its affinity of adsorbent. Several conventional isotherm equations fitted to such as Langmiur, Freundlich, Tempkin, and BET.

2.4. Freundlich isotherm

The Freundlich linear expression is an empirical equation based on multilayer sorption to a heterogeneous surface and is expressed by the following Eq. (3).

$$\log q_e = \log K_F + 1/n \log C_e \tag{3}$$

where q_e and C_e are the amount of adsorbed adsorbate per unit weight of adsorbent and unadsorbed adsorbate concentration in solution at equilibrium, respectively. K_F and $1/n$ are Freundlich constant characteristics of the system, which are determined from the Eq. (4).

$$\log q_e \text{ vs. } \log C_e \tag{4}$$

2.5. Langmuir adsorption

Langmuir monolayer adsorption isotherm is very useful for predicting adsorption capacities and also interpreting into mass transfer relationship. The isotherm can be written as follows:

$$C_e/q_e = (1/K_L) + (a_L/K_L)C_e \tag{5}$$

The constant K_L(L/g) is the Langmuir equilibrium constant, and the a_L/K_L gives the theoretical monolayer saturation capacity. These Langmuir parameters were obtained from the linear correlations between the values of C_e/q_e and C_e. Generally, the Langmuir equation applies to the cases of adsorption on completely homogeneous surfaces.

2.6. Temkin isotherm

This isotherm describes the behaviour of adsorption systems on heterogeneous surfaces and it has generally been applied in the following form:

$$q_e = B \ln A + B \ln C_e \quad (6)$$

A plot of q_e vs. ln C_e enables to determine the constants A and B.

2.7. BET method

Specific surface area, pore volume and pore size of the sample were determined by means of N_2 adsorption–desorption at −195.629°C applying the BET method.

2.8. Kinetic studies

The adsorption kinetics is important as it can predict the rate at which an As^{3+} is removed and provide valuable insights into the mechanism of sorption reactions. To study the rate constant for the adsorption of As^{3+} on ZnO-NPs-AS, the following kinetic models were tested to fit experimental data obtained. As^{3+} of initial concentration of 0.005–0.08 was treated at different contact durations of 10–80 min at pH 1–7 and adsorbent dosage of 0.5–4.5 g at an agitation of 50–400 rpm.

2.9. Pseudo-first-order equation

The pseudo-first-order equation is given as follows:

$$\ln(q_e - q_t) = \ln q_e - k_1 t \quad (7)$$

where q_t and q_e are the amounts of As^{3+} adsorbed at time t and equilibrium, respectively, and k_1 is the pseudo-first-order rate constant for the adsorption process. The linear graph of $\ln(q_e - q_t)$ vs. t shows the applicability of first-order kinetic.

2.10. Pseudo-second-order equation:

This chemisorption kinetic rate equation is expressed as follows:

$$t/q_t = (1/k_2 q_e^2) + (1/q_e)t \quad (8)$$

where k_2 is the equilibrium rate constant of pseudo-second-order equation. The linearity of t/q_t vs. t suggests the best fitted with pseudo-second-order kinetic.

2.11. Intraparticle equation

Kinetic data can also be analysed by an intraparticle diffusion kinetic model formulated as follows:

$$q_t = k_p t^{1/2} + C \quad (9)$$

where k_p is the intraparticle diffusion rate constant and C is the intercept of the plot of q_t vs. $t^{1/2}$. If this linear plot passes through the origin then intraparticle diffusion is the rate-controlling step.

2.12. Input parameters

Common isotherms are used in this investigation to generate different series of adsorption data that will serve as learning data-sets to fit ANNs. The four types of isotherms are Langmuir, Freundlich, Temkin, and BET. Langmuir isotherm applies to localized adsorption of monolayer surface coverage assuming that each adsorbed molecule occupies one adsorption site. Freundlich isotherm is a semi-empirical equation which is widely used to represent adsorption equilibrium data for low to intermediate range of concentration. Temkin isotherm describes the behaviour of adsorption systems on heterogeneous surfaces. Specific surface area, pore volume and pore size of the sample were determined by means of N_2 adsorption–desorption at −195.629°C using BET analysis. The physisorption and chemisorptions kinetic rate equation is determined using pseudo-first and second-order rate equation. Parameters such as concentration, dosage, contact time, pH and agitation have been evaluated by means of portable instruments and analysed in the laboratory. The maximum adsorption of As^{3+} is found to be 98.31% at pH 5, equilibrium time of 50 min using adsorbent of 3 g/L and initial concentration of 0.06 mg/L at agitation speed of 250 rpm. It is desired to test a three-layer neural network structure to represent the data of all simulated isotherm and kinetic data. In line with the studies carried out, multilayer perceptron with back propagation (BP) algorithm has been adopted in designing different structures of the neural network. In the multilayer neural network, depending on the pattern of relation between the materials, input is put in first layer (Xi) and the output in the last layer (y) by means of neurons weights (W), bias (b) and the activity algorithm ($f(x)$) in the middle layer(s). The network design has been grounded on a combination of information on the parameters effective on the adsorption. In each structure, the input information after processing is put through to the next layer(s) through the output of the first layer neurons and finally provided that it is acceptable to the network output. This process goes on as long as a suitable result comes out. In this study, several training algorithms and functions embedded

in the neural networks toolbox of nntool matlab software 2010a were adapted. In this research, the data have been divided into two groups randomly and based on the experiences on the part of other researches and trial and error has been taken to all stages training data, accounting for 70%training and testing data making up 30% of the total data. The sigmoid simulating tangent and linear purelin algorithms were applied in operating the neural network. Moreover, for each simulating algorithm, training rules such a Levenberg Marquate is subjugated. It is worth mentioning that the input, middle and output neuron simulating algorithms were considered identical. With regard to this, studies also implied that the simulating algorithms being the same, more satisfactory results come out, as opposed to the simulating algorithms corresponding to different layers [39–41]. The total parameters examined that the timing series run to 95 of which 67 were set aside for network training and 28 parameters have been used for the final testing and validation analysis. The adequacy of the ANN is evaluated by considering the coefficient of determination (R^2) and also the values of root mean square error (RMSE). The acceptance criterion rests on the quantitative error passing into the calculations and observations including maximum R^2 and minimum RMSE [42,43].

$$\text{RMSE} = \sqrt{\frac{\sum_{i=0}^{n} (\text{actual} - \text{pridicted})^2}{n}} \tag{10}$$

$$R^2 = 1 - \frac{\sum_{i=0}^{n} (\text{actual} - \text{pridicted})^2}{\sum_{i=0}^{n} (\text{actual} - \text{average})^2} \tag{11}$$

2.13. Optimization of the ANN structure

Neural networks have been the subject of considerable research interest for the past 20 years. ANNs attempt to mimic how a biological system functions and how they can be utilized for their novel architecture to solve highly complex undefined and non-linear mathematical problems. ANNs can simply be viewed as general non-linear models which have the ability to encapsulate the underlying relationship that exists between a series of inputs and outputs of a system. They possess a high degree of flexibility and plasticity that allows them to easily capture the non-linear behaviour of a process using input–output data. FFNNs are undoubtedly the most popular neural network structure used in engineering applications. It has been shown that a three-layer FFNN can represent any function provided that sufficient number of neurons is present. A FFNN normally consists of three layers: an input layer, a hidden layer and an output layer. The FFNNs have been used in this investigation are presented in Fig. 7. The input layer receives the process inputs and fans out this information to all functional neurons of the hidden layer. Each neuron of the hidden layer essentially performs two tasks: (1) a weighted summation of all process inputs and (2) a non-linear transformation via a neuron transfer function of the weighted summation to produce the output of each neuron of the hidden layer which then serves as inputs to the neurons of the output layer. The output layer performs the same task as the neurons of the second layer to produce the final output of the FFNN. The typical transfer functions that are used in the hidden and output layers are tansig and purelin. The output to the FFNN is usually scaled between 0 and 1 or −1 to 1. The concentration of AS $^{3+}$ ion in final solution is obtained by using the ANN model developed. The experimental values of equilibrium concentration (mg/ml), amount of adsorbate adsorbed per unit amount of adsorbent (mg/gm), agitation speed pH and % adsorption are calculated for the various dosage of adsorbent.

3. Results and discussion

3.1. FT-IR characterization of ZnO-NPs-AS

FT-IR measurements were agreed out to identify the biomolecules for capping and proficient stabilization of the metal nanoparticles synthesized by *Azadirachta* leaf extract (Fig. 1). The FTIR spectrum of zinc oxide nanoparticles absorbs at 408–550 cm^{-1} [44].

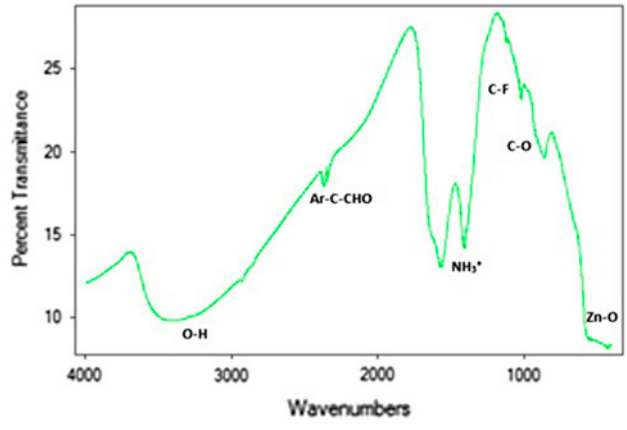

Fig. 1. FT-IR spectrum of green synthesis of *ZnO NPs* using *A. indica*.

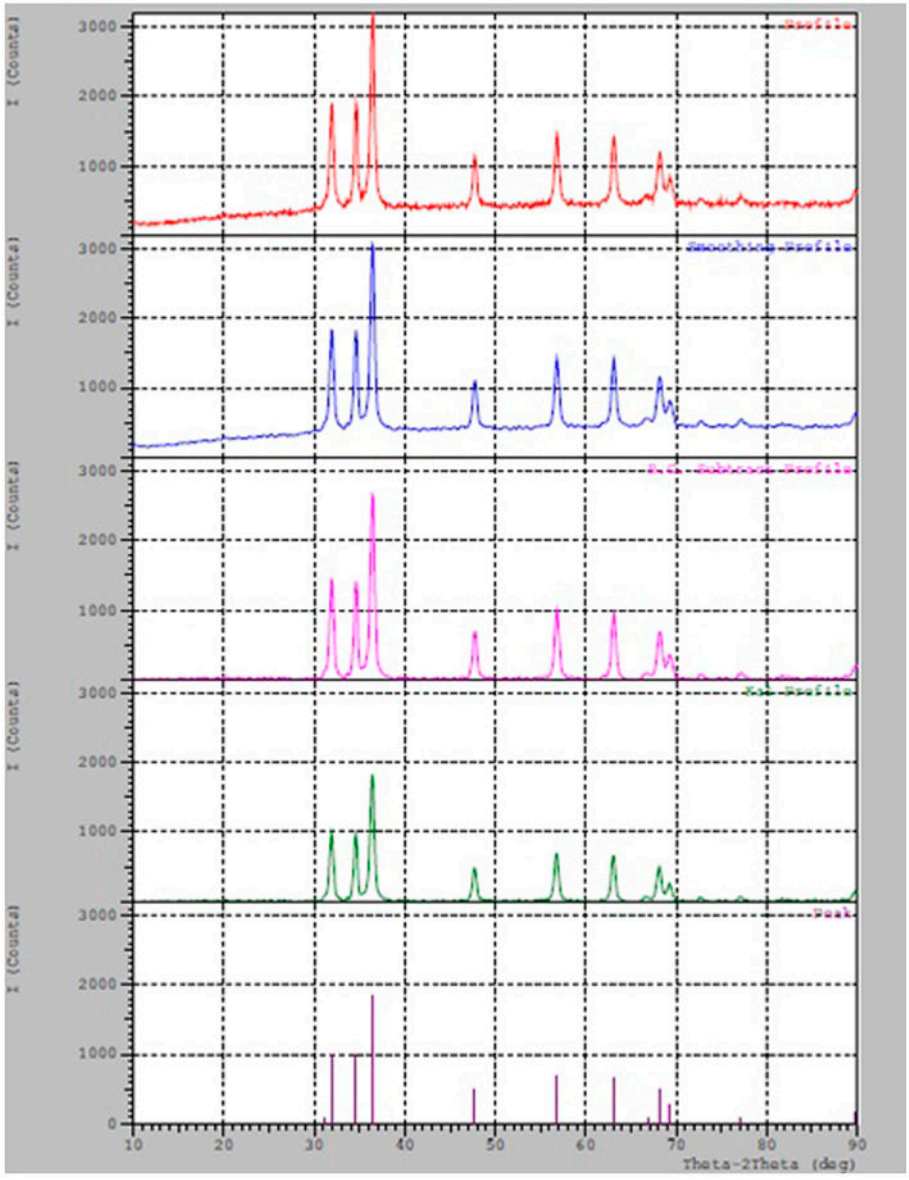

Fig. 2. Distinctive XRD characterization of ZnO-NPs-AS.

The O–H stretch appears in the spectrum as a very broad band extending from 3,400 cm $^{-1}$. This very broad O–H strech band is seen along with a C=O peak, it almost certainly indicates the compound is an aliphatic carboxylic acid. Two peaks attributed to C–F stretching at 1,105 cm^{-1} constitute mono and poly fluorinated compounds. Medium absorption in the region 1,581–1,415 cm^{-1} implies the presence of aromatic ring. The absorption peak at 1,015 cm^{-1} corresponds to C–O stretching of saturated primary alcohol. The prominent doublet absorption at 2,921 cm^{-1} indicates C–H stretching vibration of an aromatic aldehyde .The presence of this doublet allows aldehydes to be distinguished from other carbonyl-containing compounds. These bands are indicative of terpenoid group of compounds present in aqueous neem extract. Some of the major chemical constituents present in neem leaves have been identified through detailed studies using NMR, FTIR as quercetin rhamnoside (0.45%), a flavonoid quertcetin (0.257%), and nimbin (0.19%). A few other constituents are also present nimbocinone (250 ppm), nimbandiol (130 ppm) [45]. Therefore, the synthesized nanoparticles were surrounded by metabolites such as terpenoids having functional group of alcohols, ketones, aldehyde and carboxylic acids are confirmed [46].

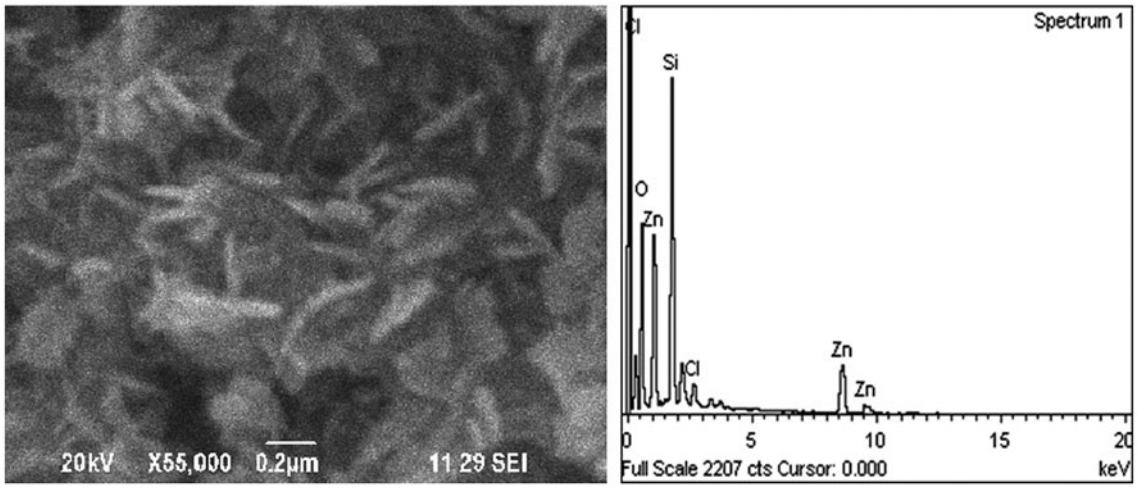

Fig. 3. Unique EDX and SEM characterization of ZnO-NPs-AS.

A distinctive XRD pattern (Fig. 2) shows the ZnO-NPs-AS prepared by the green synthesis method at 60˚C for 12 h for aqueous leaf extract of *A. indica*. It can be seen that all of these peaks are well matched with that of Zincite phase (JCPDS CARD NO: 36-1451) equivalent characteristic peak predominantly at about 12˚, 20˚ for silica and 32˚, 34˚, 36˚ for ZnO NPs are indicative of nanocrystalline nature of ZnO-NPs-AS in combination. The EDX spectrum (Fig. 3) shows the peak only for the presence of zinc, oxygen and silicon elements in the as-prepared ZnO-NPs-AS before adsorption of As^{3+}. The SEM image (Fig. 3) reveals flower-like morphology without agglomeration and particle size distribution of ZnO-NPs-AS is found to have the size ranging 100 nm (Fig. 4).

The EDX spectrum (Fig. 5) confirms the peak for the presence of zinc, oxygen, silicon and arsenic elements after adsorption of As^{3+}. In this work, several training algorithms—such as Levenberg–Marquardt BP, resilient BP, gradient descent, gradient descent with momentum BP, gradient descent with adaptive LR BP and gradient descent with momentum and adaptive LRBP—were tested to discover the optimum learning algorithm. Furthermore, several network types containing more than one hidden layer and more neurons in the input/hidden/output layers were also tested with the learning algorithms. Fig. 4 shows a feed forward back propagation (FFBP) algorithm with five dependant variables of three-layer architecture; a single hidden layer with a tangent sigmoid transfer function (tansig) at input and a linear transfer function (purelin) at output layer are used and run on nftool MATLAB 11a.The distribution of output of training data was presented in (Figs. 6 and 7) using

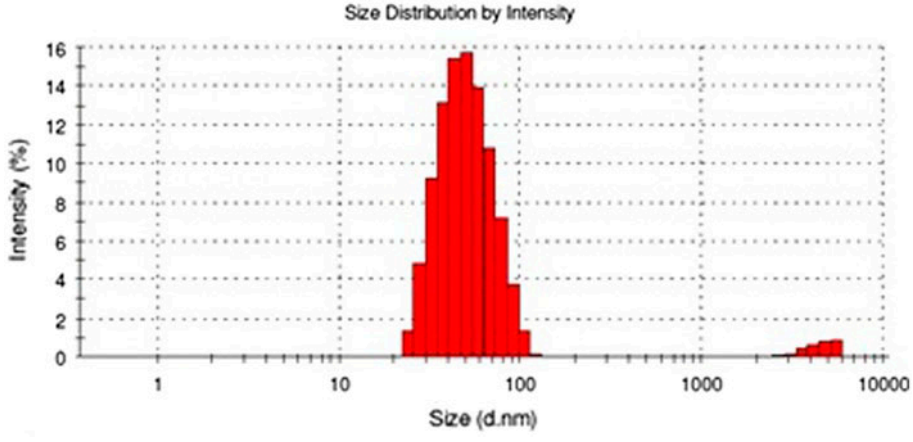

Fig. 4. Particle size distribution of ZnO-NPs-AS.

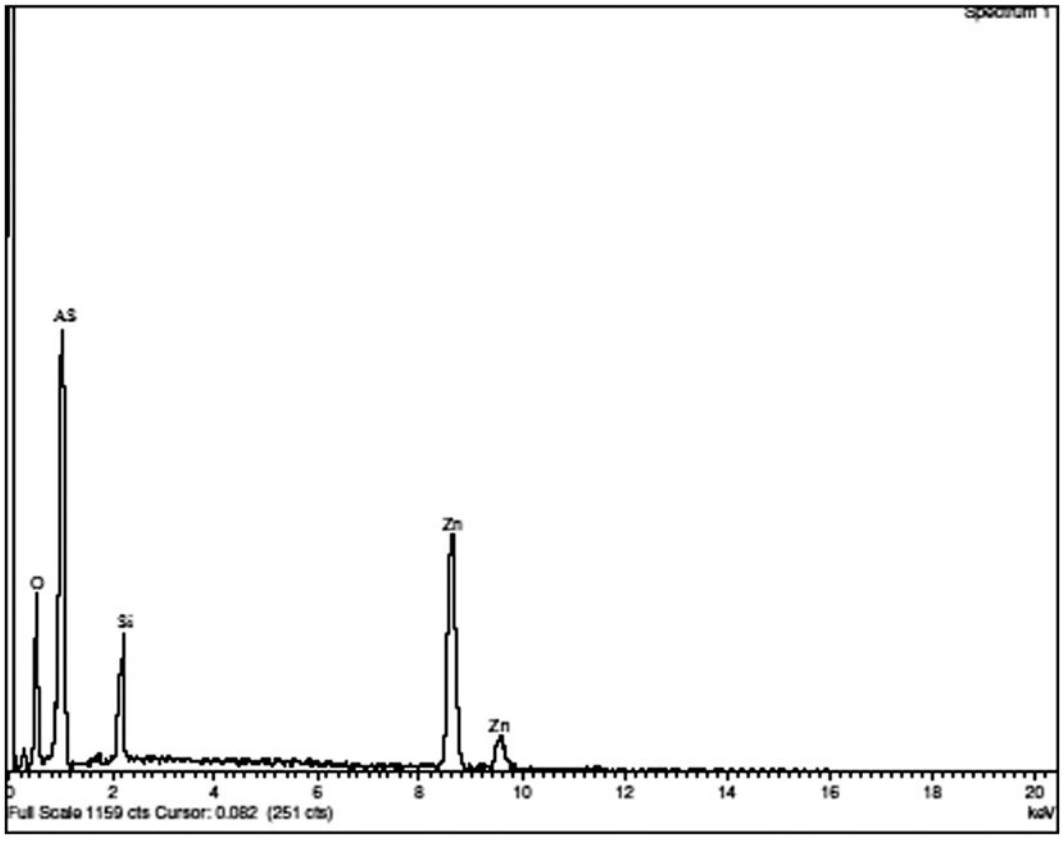

Fig. 5. Typical EDX characterization of ZnO-NPs-AS after adsorption of AS (III).

correlation coefficient (Fig. 8) and confusion matrix (Fig. 9) similarly, the minimum error was portrayed in (Fig. 10) by best validation performance and error histogram with the contribution of five inputs from (Figs. 11 and 12).

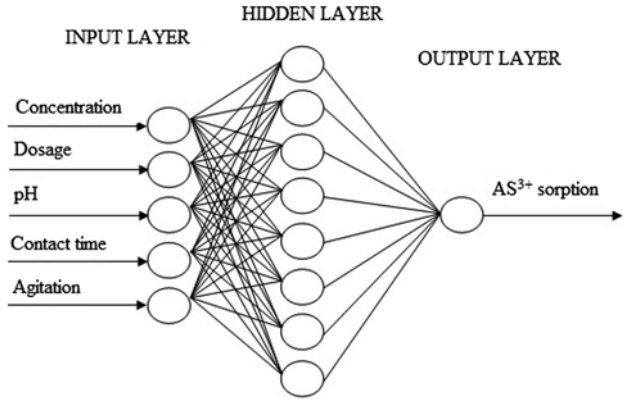

Fig. 6. Predicted ANN Architecture for five various parameters.

The experimental designs (Table 3) were used for calculating adsorption capacity in percent (removal) by changing initial concentration (mg/L), pH level, adsorbent dosage (g/L), contact time (min) and agitation (rpm) were repeated 7–12 times to increase the reliability. The feed forward three-layered multilayer neural networks used consist of hidden layer, input layer and output.

According to the basic statistical observations and the optimum network type consideration, FFBP was found to be the best one among them (Table 4).

Twenty neurons are used in the hidden layer. In the first layer or the hidden layer, the tan sigmoid transfer function as shown was used. This transfer function gives output values between −1 and +1 or 0 and 1. The tan sigmoid function takes the form, $a = 2/(1 + e^{-2n}) - 1$. In the output layer, purelin transfer function was used. This is a linear transfer function. The transfer function tan sigmoid used in the hidden layer takes up only values between −1 and 1 and gives outputs between −1 and 1 or 1 and 0. Hence, the values that are fed into the network have been scaled between −1 and +1. The algorithm used for normalization is given by:

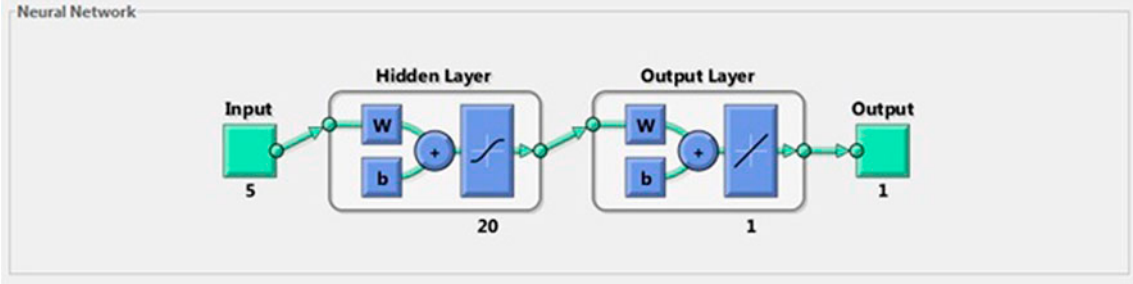

Fig. 7. LMFFBP networks for 5-20-1 type of ANN architecture.

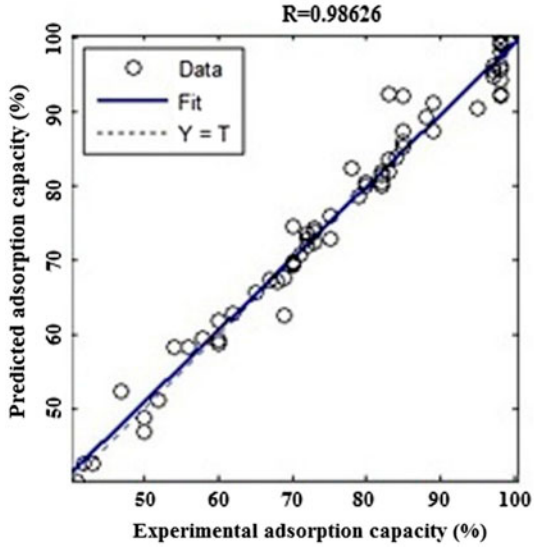

Fig. 8. Correlation of predicted and actual As^{3+} sorption percentage.

$$P_i = (p_i - p_{min})/(p_{max} - p_{min}) - 1$$

where p_{min} and p_{max} are the minimum and maximum of the input and target values, respectively. Fig. 5 predicts the sorption efficiency with reasonable accuracy 1. For the present study, a total of 95 points have been used to train the neural network, of which 67 points are chosen for training and 14 points are chosen for validation and 14 points for testing. Total iteration number was set as 1,000 at 22 epochs for all learning algorithms and the performance goal is set at 10^{-5}. A Feed Forward BP was used for modelling the experimental design for predicting the removal capacity of As^{3+}. The experimental design used in this research work was based on one factor experiment at a time. The data and their related statistics are given in Table 5.

The network is tested with different number of neurons to find the optimal number of neurons at the hidden layer by observing the mean squared error (MSE). Twenty neurons are selected in the hidden layer when mean squared error starts decreasing. Learning and momentum parameters are set at 0.30 and 0.20, respectively, during the training phase. During training phase, the output vector is computed by a forward pass in which the input is propagated forward through the network to compute the output value of each unit. The output vector is then compared with the desired vector which resulted into error signal for each output unit. In order to minimize the error, appropriate adjustments were made for each of the weights of the network. After several such iterations, the network was trained to give the desired output for a given five input vector. Then, network is trained till minimum root mean square error is observed (Table 5) A root mean square error of 0.0014 is observed at epoch number 22 (Fig. 10). Training was stopped at this point and weights have been frozen for network to undergo testing phase. A high degree of correlation between actual and predicted sorption efficiency of 100% observed is shown in Fig. 8 with high coefficient of determination (R^2 = 0.986) is obtained. When the network is well trained, testing of the network with testing data-set is carried out. A high degree of correlation (100%) between output and input sorption efficiency (mg/g) is observed as shown in Fig. 9. The average absolute relative percentage is observed in Fig. 13.

The mathematical isotherm and kinetic models approximating (Figs. 14–19) Langmuir, Freundlich, Temkin, pore volume, pseudo-first order, pseudo-second order of the present study have been compared to ANN. The Table 4 predicts the equilibrium adsorption behaviour of ZnO nanoparticle entrenched on activated silica with a good degree of accuracy with ANN of maximum R^2 (0.986) and minimum MSE (0.0014) in contrast with other mathematical isotherm and kinetics. The development of the proposed ANN model is an effort

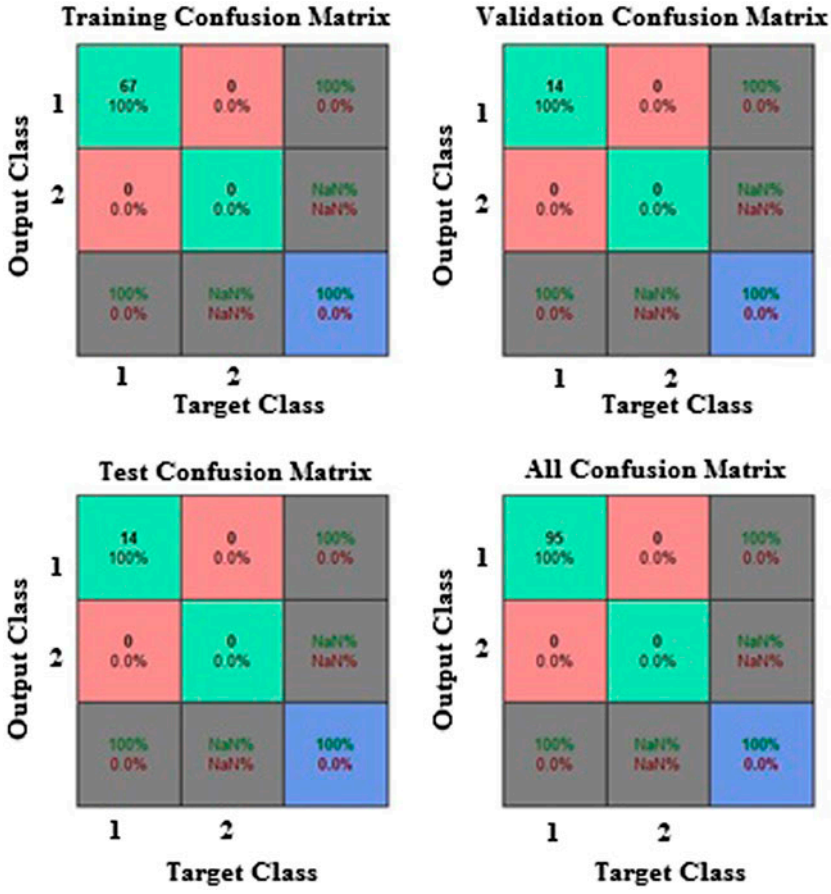

Fig. 9. Confusion matrix output for input to training testing and validation.

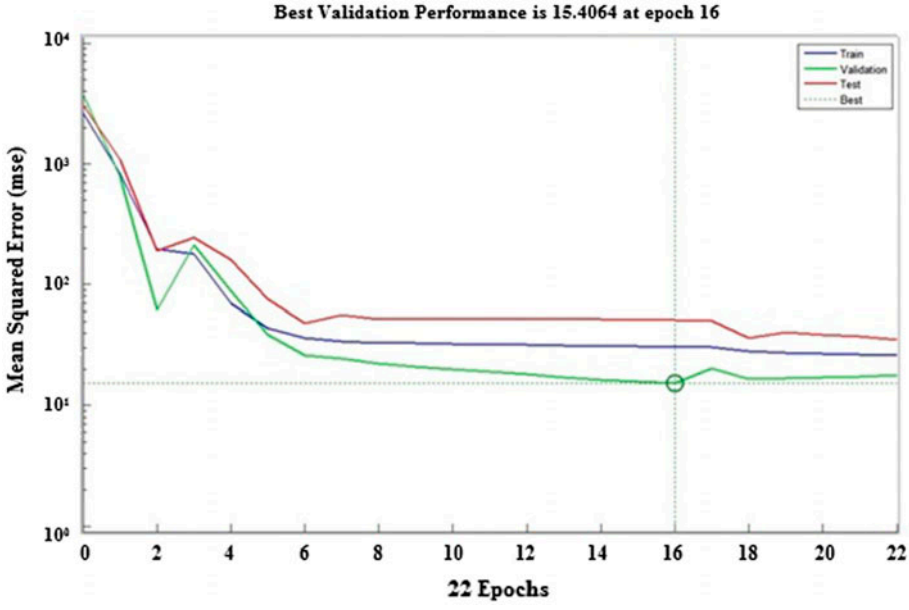

Fig. 10. The mean absolute relative percentage error for training data.

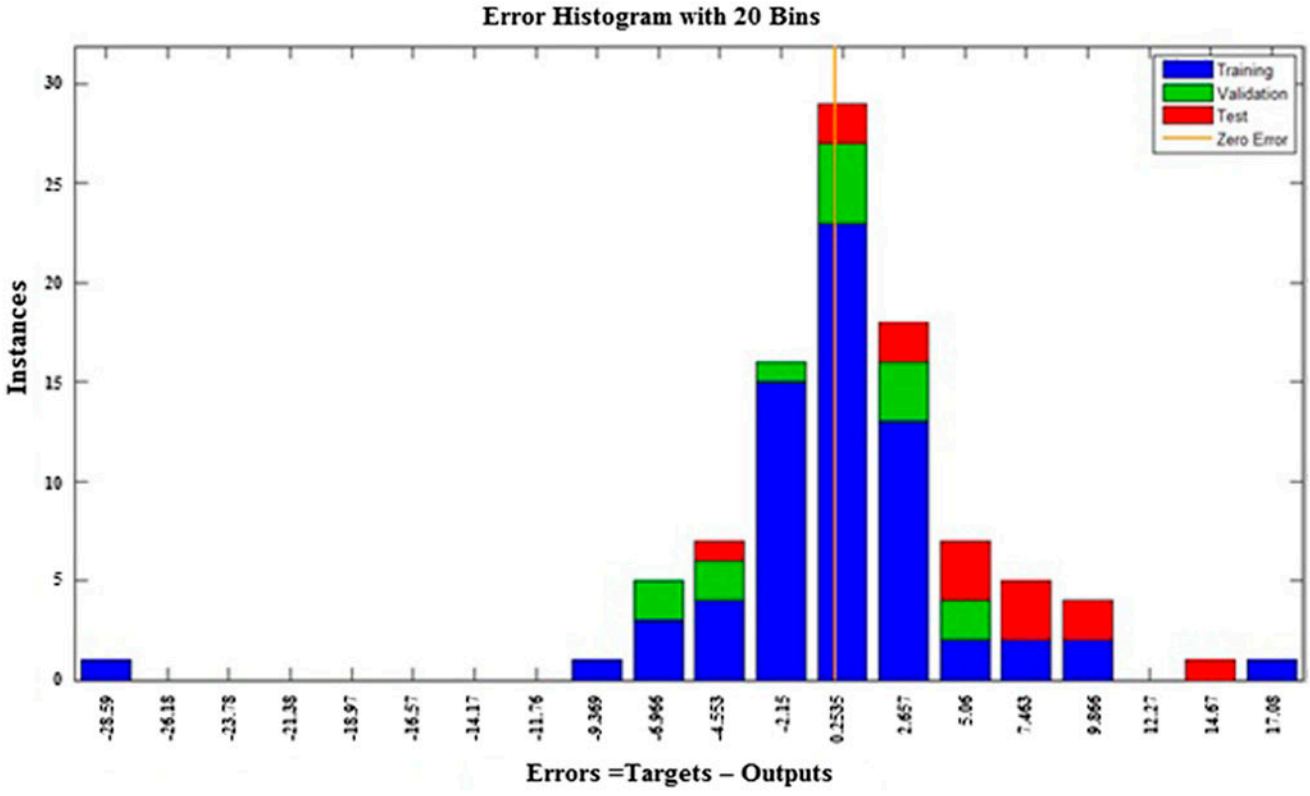

Fig. 11. Zero error histogram for training.

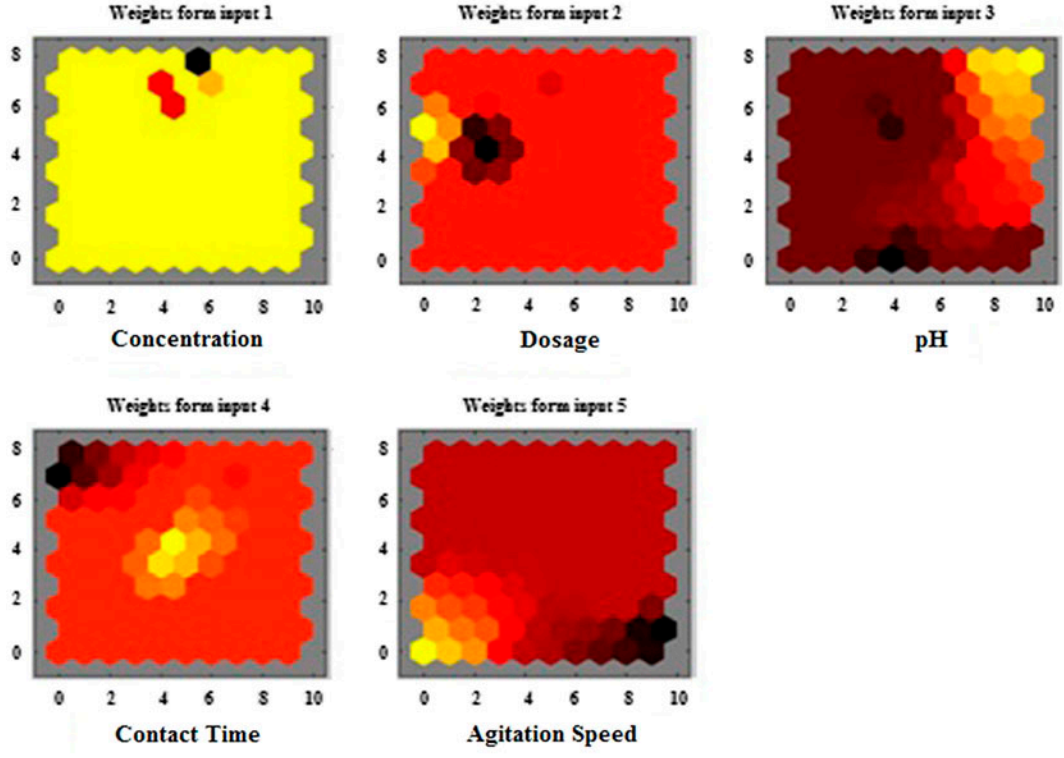

Fig. 12. Component planes and U matrix visualization of five input layer.

Table 3
Experimental design for removal of As^{3+} using ZnO-NPs-AS

Input variable	No. of runs	Range	Average removal %
Concentration	7	0.0075–0.10	74.61
Adsorbent dosage	10	0.5–5.5	85.81
Contact time	12	10–120	86.81
Initial pH	7	2–8	72.14
Agitation	10	50–500	75.49

Table 4
Empirical and mathematical correlations in the prediction of adsorption

S. No.	Models	R^2	MSE
1	Artificial neural network (training)	0.986	0.0014
2	Langmuir	0.974	0.0025
3	Freundlich	0.897	0.021
4	Temkin	0.943	0.006
5	Pseudo first order	0.132	72.95
6	Pseudo second order	0.906	0.001
7	Intra particle diffusion	0.806	0.053
8	Testing	0.984	0.0019
9	Validation	0.976	0.0021

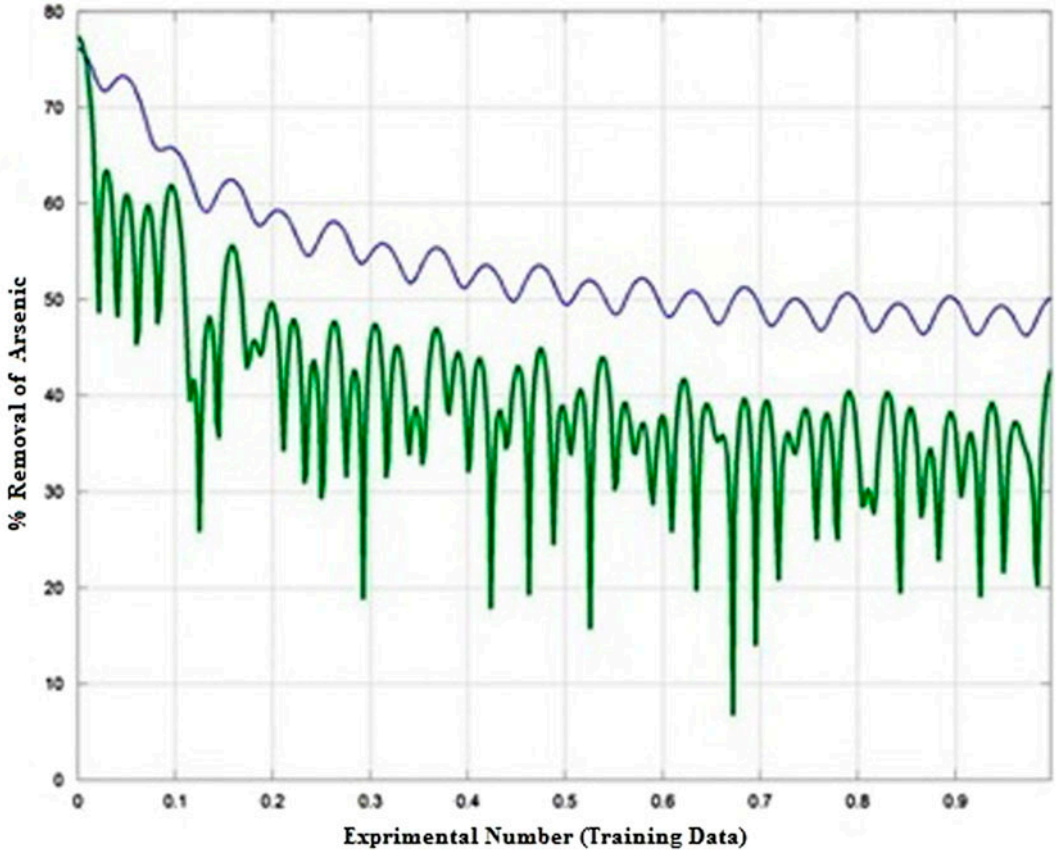

Fig. 13. Figure average distribution of As^{3+} removal % for training data.

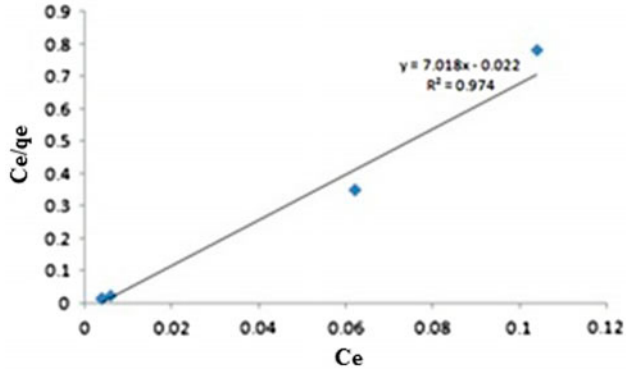

Fig. 14. Langmiur adsorption isotherm for As^{3+} using ZnO-NPs-AS.

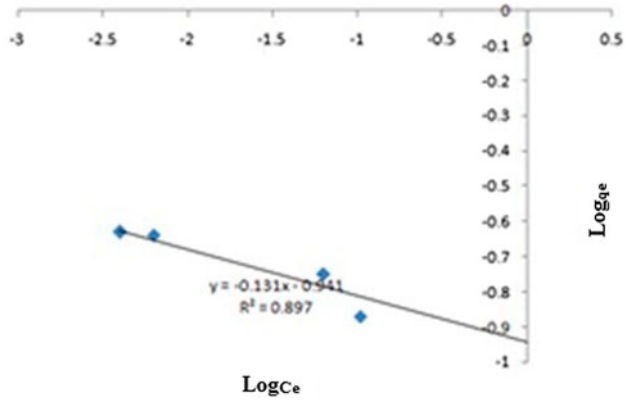

Fig. 15. Freundlich adsorption isotherm for removal of As^{3+} using Zno-NPs-AS.

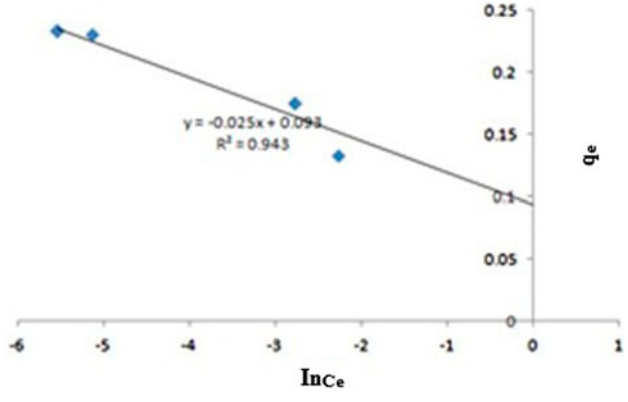

Fig. 16. Tempkin adsorption isotherm for As^{3+} using ZnO-NPs-AS.

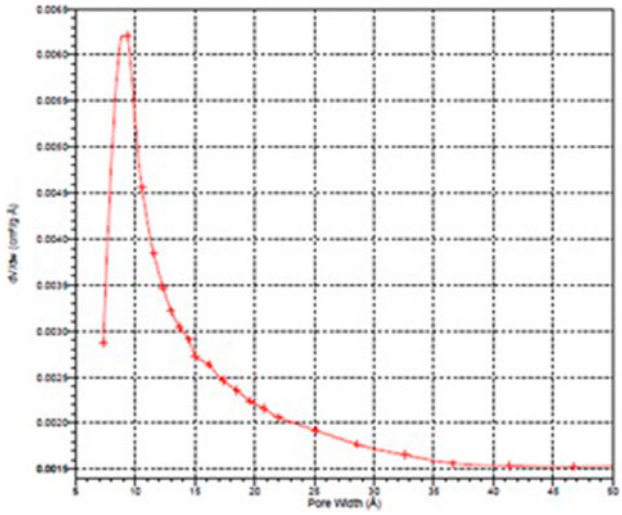

Fig. 17. Pore volume plot.

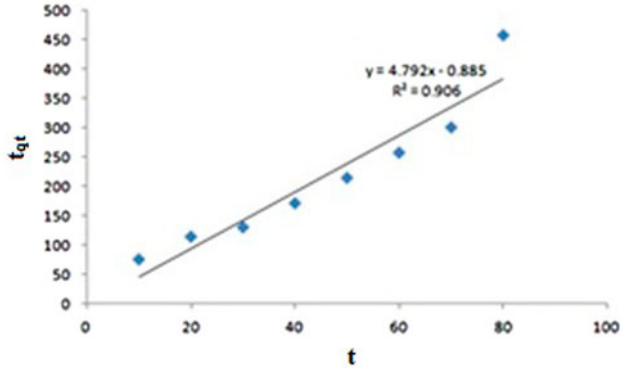

Fig. 18. Pseudo second order kinetic for adsorption of As^{3+} using ZnO-NPs-AS.

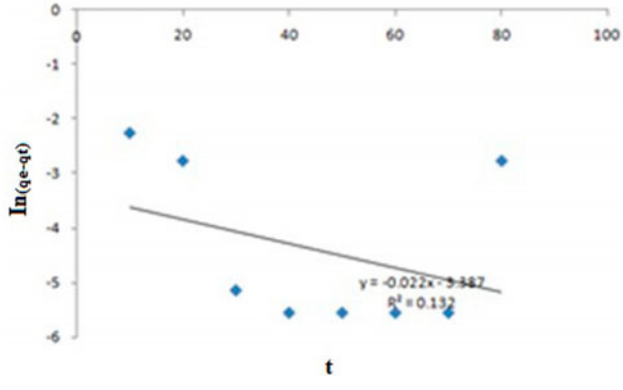

Fig. 19. Pseudo first order kinetic for adsorption of As^{3+} using ZnO-NPs-AS.

Table 5
The performance of LMFFBP Network for 5-20-1 type of ANN

Training algorithm	Max (RMSE)	Min (RMSE)	Max (R^2)	Min (R^2)
Levenberg-Marquardt	0.0789	0.0014	1	0.986

towards the growing interest in applying ANN modelling technique to the area of adsorption of As^{3+} from aqueous solutions. Obeying pseudo-second-order kinetics (Fig. 12) i.e. the rate of the reaction depends upon the third and fifth parameter among the five parameters which was an authentication for experimental proof. The studies conclude that ANN approach is quite efficient in modelling complex adsorption phenomenon.

4. Conclusion

- Introduction of this knowledge-based system is efficient and this green approach confirmed the prediction of percentage adsorption efficiency for the removal of As (III) ions.
- The present piece of work demonstrates the successful removal of As (III) ions from the aqueous solutions using *A. indica* (ZnO-NPs-As-*Os*) with maximum removal efficiency (98.31%).
- Adsorption equilibrium data were best described by Langmuir isotherm and BET model and fit quite well with the experimental data accomplished that the maximum adsorption corresponds to a saturated monolayer of As^{3+} molecules on the adsorbent surface with constant energy.
- The data were analysed using kinetics models akin to pseudo-first and second order and the findings presented in this study suggested following pseudo-second-order equation for the adsorption of As^{3+} on to Zno-NPs-AS.
- The three-layered (5-20-1) ANN modelling technique was applied to optimize this experimental process.
- The Levenberg–Marquardt algorithm was found best of BP algorithms with a minimum MSE for training is 0.0014, respectively. The maximum removal As (III) ions of 100% is obtained at concentration of 0.006 mg/L, absorbent dosage to 3 g, contact time 50 min and agitation speed of 250 rpm at pH5.
- The correlation coefficient (R = 0.98626) confirms the degree of linear dependence of two random variables when compared to the classic model.
- The present outcome recommends that ZnO-NPs-AS-*Os* synthesized in an ingenious green method may be used as an economical and effectual adsorbent for the confiscation of As (III) ions from aqueous solutions.
- The power of the proposed neural isotherm models lies in the universality of its application. The ability of a single unifying model capable of representing data for all recognized types of adsorption isotherm models is an achievement that classic adsorption isotherm models cannot attain individually.

References

[1] J. Matschullat, Arsenic in the geosphere—A review, Sci. J. Total Environ. 249 (2002) 297–312.
[2] P.L. Smedley, D.G. Kinniburgh, Source and behaviour of arsenic in natural waters, in: United Nations Synthesis Report on Arsenic in Drinking Water, British Geological Survey, Wallingford, Oxon, 2005 (Chapter 1).
[3] D. Ranjan, M.H. Talat, S.H. Hasan, Biosorption of arsenic from aqueous solution using agricultural residue 'rice polish', J. Hazard. Mater. 166 (2009) 1050–1059.
[4] S.Y. Thomas, T.G. Choong, Y. Robiah, F.L. Gregory Koay, I. Azni, Arsenic toxicity, health hazards and removal techniques from water: An overview, Desalin. Water Treat. 217 (2007) 139–166.
[5] S. Wang, C.N. Mulligan, Speciation and surface structure of inorganic arsenic in solid phases: A review, Environ. Int. 34 (2008) 867–879.
[6] A.H. Smith, P.A. Lopipero, M.N. Bates, C.M. Steinmaus, Arsenic epidemiology and drinking water standards, Science 296(5576) (2002) 2145–2146.
[7] M. Zaw, M.T. Emett, Arsenic removal from water using advanced oxidation processes, Toxicol. Lett. 133 (2002) 113–118.
[8] F.S. Zhang, H. Itoh, Iron oxide-loaded slag for arsenic removal from aqueous system, Chemosphere. 60 (2005) 319–325.
[9] N. Balasubramanian, T. Kojima, C. Basha, C. Srinivasakannan, Removal of arsenic from aqueous solution using electrocoagulation, J. Hazard. Mater. 167 (2009) 966–969.
[10] G. Ghurye, L. Clifford, D.A. Tripp, Combined arsenic and nitrate removal by ion exchange, J. Am. Water Works Assoc. 91(10) (1999) 85–96.
[11] S. McNeill, M. Edwards, Predicting arsenic removal during metal hydroxide precipitation, J. Am. Water Works Assoc. 89 (1997) 75–82.
[12] D.H. Kim, K.W. Kim, J. Cho, Removal and transport mechanisms of arsenics in UF and NF membrane processes, J. Water Health 4(2) (2006) 215–223.

[13] P. Kumari, P. Sharma, S. Srivastava, M.M. Srivastava, Biosorption studies on shelled Moringa oleifera Lamarck seed powder: Removal and recovery of arsenic from aqueous system, Int. J. Miner. Process. 78 (2006) 131–139.
[14] V.K. Sharma, M. Sohn, Aquatic arsenic: Toxicity, speciation, transformations and remediation, Environ. Int. 35 (2009) 743–759.
[15] F. Mjalli, S. Al-Asheh, F. Banat, N. Al-Lagtah, Representation of adsorption data for isopropanol-water system using neural network techniques, Chem. Eng. Technol. 28(12) (2005) 1529–1539.
[16] S. Ridvan, Y. Nalan, D. Adil, Biosorption of cadmium, lead, mercury, and arsenic ions by the fungus Penicillium purpurogenum, Sep. Sci. Technol. 38(9) (2003) 2039–2053.
[17] D. Pokhrel, T. Viraraghavan, Arsenic removal from an aqueous solution by modified *A. niger* biomass: Batch kinetic and isotherm studies, J. Hazard. Mater. 150 (2007) 818–825.
[18] T. Kamala, K.H. Chu, N.S. Chary, P.K. Pandey, S.L. Ramesh, A.R.K. Sastry, K. Sekhar, Removal of arsenic (III) from aqueous solutions using fresh and immobilized plant biomass, Water Res. 39(13) (2005) 2815–2826.
[19] G.S. Murugesan, M. Sathishkumar, K. Swaminathan, Arsenic removal from groundwater by pretreated waste tea fungal biomass, Bioresour. Technol. 97(3) (2006) 483–487.
[20] T. Akar, S. Tunali, I. Kiran, *Botrytis cinerea* as a new fungal biosorbent for removal of Pb(II) from aqueous solutions, Biochem. Eng. J. 25 (2005) 235–243.
[21] A. Gupta, V.S. Chauhan, N. Sankararamakrishnan, Preparation and evaluation of iron–chitosan composites for removal of As(III) and As(V) from arsenic contaminated real life groundwater, Water Res. 43 (2009) 3862–3870.
[22] M. Sen, A. Manna, P. Pal, Removal of arsenic from contaminated groundwater by membrane-integrated hybrid treatment system, J. Membr. Sci. 354 (2010) 108–113.
[23] A.Ö.A. Tuna, E. Özdemir, E.B. Şimşek, U. Beker, Removal of As(V) from aqueous solution by activated carbon-based hybrid adsorbents: Impact of experimental conditions, Chem. Eng. J. 223 (2013) 116–128.
[24] A.I. Okoye, P.M. Ejikeme, O.D. Onukwuli, Lead removal from wastewater using fluted pumpkin seed shell activated carbon: Adsorption modeling and kinetics, Int. J. Environ. Sci. Tech. 7(4) (2010) 793–800.
[25] H. Basu, K. Biswas, Prediction of gasphase adsorption isotherms using neural nets, Can. J. Chem. Eng. 80 (2002) 1–7.
[26] D. Gnanasangeetha, D. SaralaThambavani, Green synthesis and characterisation of biocompatible zinc oxide nanoflowers using *azadirachta indica*, Elixir. NanoTech. 62 (2013) 17594–17598.
[27] D. Gnanasangeetha, D. SaralaThambavani, Biogenic Production of Zinc Oxide Nanoparticles Using *Acalypha indica*, J. Chem. Biol. Phys. Sci. 2(4) (2014) 238–246.
[28] D. Gnanasangeetha, D. SaralaThambavani, Benign ZnO Nanoparticle as a practical adsorbent for removal of As^{3+} embedded on activated silica using *Ocimum Sanctum*, Discovery 16(46) (2014) 33–41.
[29] W. Gao, S. Engell, Neural-network based identification of nonlinear adsorption isotherms, in: Dynamics and Control of Process Systems, Elsevier IFAC Publications, Cambridge, MA, 2004, pp. 721–724.
[30] S. Giraudet, P. Pré, H. Tezel, P. Le Cloirec, Estimation of adsorption energies using physical characteristics of activated carbons and VOCs' molecular properties, Carbon 44 (2006) 1873–1883.
[31] E.N. Vasina, E. Paszek, D.V. Nicolau, The BAD project: data mining, database and prediction of protein adsorption on surfaces. Lab Chip 9 (2009) 891–900.
[32] J.A. Anderson, An Introduction to Neural Networks, Prentice-Hall, New Delhi, 1999.
[33] R.N. Shinde, A.K. Pandey, R. Acharya, R. Guin, S.K. Das, N.S. Rajurkar, P.K. Pujari, Chitosan-transition metal ions complexes for selective arsenic(V) preconcentration, Water Res. 47 (2013) 3497–3506.
[34] O.M. Vatutsina, V.S. Soldatov, V.I. Sokolova, J. Johann, M. Bissen, A. Weissenbacher, A new hybrid (polymer/inorganic) fibrous sorbent for arsenic removal from drinking water, React. Funct. Poly. 67 (2007) 184–201.
[35] A.Ö.A. Tuna, E. Özdemir, E.B. Şimşek, U. Beker, Removal of As(V) from aqueous solution by activated carbon-based hybrid adsorbents: Impact of experimental conditions, Chem. Engg. J. 223 (2013) 116–128
[36] H.A. Awala, M.M. El jamel, Equilibrium and kinetic study of adsorption of some dyes onto fledspar, J. Univ. Chem. Tech. Metal. 46(1) (2011) 45–52.
[37] D.E. Rumelhart, J.L. McClelland (Eds.), Parallel Distributed Processing, vol. 1, MIT Press, Cambridge, 1986 (Chapter 8).
[38] S.L. Pandharipande, Artificial Neural Network (FFEBPN): Elite-ANN Software CD with Case Studies, Central Techno Publishers (Denett), Nagpur, 2004.
[39] P.D. Sreekanth, N. Geethanjali, P.D. Sreedevi, Shakeel Ahmed, N. Ravi Kumar, P.D. Kamala Jayanthi, Forecasting groundwater level using artificial neural networks, Curr. Sci. 96(7) (2009) 933–939.
[40] Z. Abyaneh, B. Varkeshi, D. Arasteh, Forecasting nitrate concentration in groundwater using artificial neural network and linear regression models, Int. Agrophys. 25(2) (2011) 187–192.
[41] A.R. Tahmasebi, S.M.A. Zomorrodian, Estimation of soil liquefaction potential using artificial neural network, Second National Student Conference on Water and Soil Resources, 2004.
[42] A. Asghari Moghaddam, A. Nadiri, E. Fijani, Ability to study different models of artificial neural networks to evaluate groundwater water level in the hard formation, in: Tenth Conference of Geological Society, Tehran, 2006.
[43] A.K. Babaheydari, M. Salavati-Niasari, A. Khansari, Solvent-less synthesis of zinc oxide nanostructures from Zn(salen) as precursor and their optical properties, Particuology 10 (2012) 759–764.
[44] W.D. Perkins, Fourier transform infrared spectroscopy. Part II. Advantages of FT-IR, J. Chem. Edu. 64 (1987) A269–271.
[45] S. Siddiqui, B.S. Siddiqui, T. Mahmood, Isolation of a triterpenoid from *Azadirachta indica*, Phytochemistry, 25 (1986) 2183–2185.
[46] D. Gnanasangeetha, D. SaralaThambavani, Neural network modeling and sorption of As III with zinc oxide nanoparticle bounded on activated silica using *Ocimum sanctum*, Int. J. Engg. Sci. Res. Tech. 3(5) (2014) 206–213.